5.1 Average fidelity & averaged channel

In this section, we discuss the concepts of average fidelity and averaged channel. We also introduce briefly a technique known as twirling, which will be explored in more details in the next section. We first start by explaining what are the types of quantum channels under consideration, and we then define the notions of average fidelity and averaged channel. Finally, we give a simple expression for calculating the average fidelity.

We start with some definitions. In this work, $\mathcal{P}_n$ denotes the *n-qubit Pauli group*

$$\mathcal{P}_n := \left\{ \bigotimes_{j=1}^{n} P_j \;\middle|\; P_j \in \{I,\ X,\ Y,\ Z\} \right\}, \tag{5.1}$$

where I, X, Y and Z are the usual single qubit Pauli matrices. Also, the *weight* of an operator $P \in \mathcal{P}_n$ is denoted $\mathrm{wt}(P)$ and is defined as the number of non identity terms in its tensor product form, *e.g.* $\mathrm{wt}(I \otimes X) = 1$. Finally, the *quantum channels* under consideration in this work will be completely positive maps of the form

$$\Lambda(\rho) = \sum_{P_i, P_j \in \mathcal{P}_n} [\chi]_{ij} P_i \rho P_j, \tag{5.2}$$

where ρ is a density matrix, and χ is a matrix of dimension $4^n \times 4^n$ with $\mathrm{tr}(\chi) = 1$, $[\chi]_{ii} \geq 0$, and $[\chi]_{ij} = [\chi]_{ji}{}^*$. By convention, we will always have $P_0 := I^{\otimes n}$. Also, quantum channels with a diagonal χ matrix will be called *Pauli channels*.

We now introduce the concept of *average fidelity*. First, the *gate fidelity* between two superoperators $\mathcal{U}$ and $\tilde{\mathcal{U}}$ with respect to a state $|\psi\rangle$ is defined as

$$F_{|\psi\rangle}(\mathcal{U}, \tilde{\mathcal{U}}) = \langle\psi|\mathcal{U}^\dagger \circ \tilde{\mathcal{U}}(|\psi\rangle\langle\psi|)|\psi\rangle. \tag{5.3}$$

To get an expression independent of $|\psi\rangle$, we average over a unitarily invariant distribution of pure states to obtain the average fidelity between $\mathcal{U}$ and $\tilde{\mathcal{U}}$

$$\bar{F}(\mathcal{U}, \tilde{\mathcal{U}}) = \int d\mu(\psi) \langle\psi|\mathcal{U}^\dagger \circ \tilde{\mathcal{U}}(|\psi\rangle\langle\psi|)|\psi\rangle, \tag{5.4}$$

where $d\mu(\psi)$ is the unitarily invariant distribution of pure states known as the *Fubini-Study measure* [55]. We are interested in the noisy part of $\tilde{\mathcal{U}}$, so we define

$$\tilde{\mathcal{U}} = \Lambda \circ \mathcal{U}, \tag{5.5}$$

where Λ is the channel representing the undesired part of the evolution. It follows that

$$\bar{F}(\mathcal{U}, \tilde{\mathcal{U}}) = \int d\mu(\psi) \langle\psi|\mathcal{U}^\dagger \circ \Lambda \circ \mathcal{U}(|\psi\rangle\langle\psi|)|\psi\rangle = \int d\mu(\psi) \langle\psi|\Lambda(|\psi\rangle\langle\psi|)|\psi\rangle, \tag{5.6}$$

where the last equality is due to the fact that $d\mu(\psi)$ is unitarily invariant. We see that the average fidelity depends only on the error channel Λ, *i.e.* $\bar{F}(\mathcal{U},\tilde{\mathcal{U}}) = \bar{F}(\Lambda)$. Also, a random state can be generated from a fixed state by applying a random unitary. Thus, we can equivalently average over a distribution of random unitaries invariant under conjugation

$$\bar{F}(\Lambda) = \int d\mu(V)\langle\psi|\mathcal{V}^\dagger \circ \Lambda \circ \mathcal{V}(|\psi\rangle\langle\psi|)|\psi\rangle, \tag{5.7}$$

where $d\mu(V)$ is a unitarily invariant distribution of random unitaries known as the *Haar measure* [55]. Defining the *averaged channel* as

$$\bar{\Lambda} = \int d\mu(V)\mathcal{V}^\dagger \circ \Lambda \circ \mathcal{V}, \tag{5.8}$$

one can see that the average fidelity of Λ is in fact the gate fidelity of $\bar{\Lambda}$ with respect to the identity operation. The channel $\bar{\Lambda}$ is also known as the *Haar twirl* of Λ.

It is possible to obtain an analytical expression for the average gate fidelity. The starting point is to find a set of unitary gates $\{V_i\}$ and a probability distribution $\Pr(V_i)$ such that

$$\bar{F}(\Lambda) = \int d\mu(V)\langle\psi|\mathcal{V}^\dagger \circ \Lambda \circ \mathcal{V}(|\psi\rangle\langle\psi|)|\psi\rangle = \sum_i \Pr(V_i)\langle\psi|\mathcal{V}_i^\dagger \circ \Lambda \circ \mathcal{V}_i(|\psi\rangle\langle\psi|)|\psi\rangle. \tag{5.9}$$

Such mathematical objects are called *unitary 2-designs*, and one example of them is the n-qubit Clifford group $\mathcal{C}_n$ [56]. In other words, averaging over $\mathcal{C}_n$ and averaging over the Haar measure lead to the same average fidelity. When we average a channel Λ over the Clifford group $\mathcal{C}_n$, it can be shown that the averaged channel, denoted $\bar{\Lambda}_{\mathcal{C}_n}$, acts as [57]

$$\bar{\Lambda}_{\mathcal{C}_n}(|\psi\rangle\langle\psi|) = p|\psi\rangle\langle\psi| + (1-p)\frac{I^{\otimes n}}{2^n}, \tag{5.10}$$

where $p = \frac{4^n[\chi]_{00}-1}{4^n-1}$. Calculating the gate fidelity of $\bar{\Lambda}_{\mathcal{C}_n}$ with respect to the identity operator, we find that the average fidelity of Λ is given by [57]

$$\bar{F}(\Lambda) = \frac{2^n[\chi]_{00}+1}{2^n+1}. \tag{5.11}$$

Therefore, an estimate of the average fidelity can be obtained by measuring $[\chi]_{00}$.

In this section, we have presented the concepts of average fidelity and averaged channel. We also showed that by averaging over the n-qubit Clifford group, we can obtain a simple formula for calculating the average fidelity. According to this formula, in order to estimate the average fidelity of some quantum channel, we need to estimate $[\chi]_{00}$. How can we measure $[\chi]_{00}$ is practice? This is the topic of the next section, where we will show that this can be achieved via a technique known as twirling.

5.2 Twirling

In this section, we present the twirling protocol introduced by O. Moussa [58], and we show how it allows us to estimate the average fidelity of Clifford gates. We first introduce a new group of unitary gates, denoted $\mathcal{C}_1\Pi$. Then, we average an error channel Λ over this group, and we show that $[\chi]_{00}$ can be written as a linear combination of the eigenvalues of the averaged channel $\bar{\Lambda}_{\mathcal{C}_1\Pi}$. Finally, we show precisely how these eigenvalues can be measured experimentally for NMR systems in particular.

The group $\mathcal{C}_1\Pi$ is defined as the composition of Π_n and $\mathcal{C}_1^{\otimes n}$, where Π_n is the group of permutation of n qubits and $\mathcal{C}_1^{\otimes n}$ is the n fold tensor product of the 1-qubit Clifford group. The $\mathcal{C}_1\Pi$ twirl of a channel Λ is denoted $\bar{\Lambda}_{\mathcal{C}_1\Pi}$, and is defined as

$$\bar{\Lambda}_{\mathcal{C}_1\Pi} = \frac{1}{|\mathcal{C}_1\Pi|} \sum_{\mathcal{V}_i \in \mathcal{C}_1\Pi} \mathcal{V}_i^\dagger \circ \Lambda \circ \mathcal{V}_i. \tag{5.12}$$

It can be seen that twirling over $\mathcal{C}_1\Pi$ transforms Λ into a Pauli channel with error probabilities depending only on the weight of the error. In fact, it can be shown that [57]

$$\bar{\Lambda}_{\mathcal{C}_1\Pi}(\rho) = \sum_{\omega=0}^{n} \Pr(\omega) \mathcal{M}_\omega^p(\rho), \tag{5.13}$$

where $\Pr(\omega)$, the probability that a Pauli error of weight ω occurs, and $\mathcal{M}_\omega^p$ are given by

$$\Pr(\omega) = \sum_{\mathrm{wt}(P_i \in \mathcal{P}_n)=\omega} [\chi]_{ii}, \qquad \mathcal{M}_\omega^p(\rho) = \frac{1}{3^\omega \binom{n}{\omega}} \sum_{\mathrm{wt}(P_i \in \mathcal{P}_n)=\omega} P_i \rho P_i. \tag{5.14}$$

In particular, we have $\Pr(0) = [\chi]_{00}$. We see from Eq.(5.11) that we only need to measure the probability of no error $\Pr(0)$ in order to get an estimate of the average fidelity.

The problem of measuring the average fidelity has been translated into the problem of measuring the probability of no error. How do we measure $\Pr(0)$ in practice? First, we have to make the observation that the elements of $\mathcal{P}_n$ are eigenoperators of $\bar{\Lambda}_{\mathcal{C}_1\Pi}$. This can be understood from Eq.(5.14) and the fact that Pauli operators either commute or anti-commute with each other. In fact, it can be demonstrated that [57]

$$\bar{\Lambda}_{\mathcal{C}_1\Pi}(P) = \lambda_\omega P, \quad \text{where } P \in \mathcal{P}_n \text{ and } \omega = \mathrm{wt}(P). \tag{5.15}$$

The eigenvalues $\{\lambda_\omega\}$ are real numbers in the interval $[-1, 1]$ and depend only on the weight of their associated Pauli operator [57]. By default, we have $\lambda_0 = 1$. It can be

demonstrated that the relationship between the $\{\lambda_\omega\}$ and the $\{\Pr(\omega)\}$ is [57]

$$\lambda_\omega = \sum_{\omega'=0}^{n} [\Omega]_{\omega,\omega'} \Pr(\omega'), \qquad \Pr(\omega) = \sum_{\omega'=0}^{n} [\Omega^{-1}]_{\omega,\omega'} \lambda_{\omega'}, \tag{5.16}$$

where the matrices Ω and Ω^{-1} are given by [57]

$$[\Omega]_{\omega,\omega'} = \left[\sum_{L=0}^{n} \frac{\binom{n-\omega}{\omega'-L}\binom{\omega}{L}}{\binom{n}{\omega'}} \frac{3^L + (-1)^L}{3^L} \right] - 1 \tag{5.17}$$

$$\left[\Omega^{-1}\right]_{\omega,\omega'} = \frac{3^{\omega+\omega'}\binom{n}{\omega}\binom{n}{\omega'}}{4^n} [\Omega]_{\omega,\omega'}. \tag{5.18}$$

In particular, for $\Pr(0)$, this implies that

$$\Pr(0) = \sum_{\omega=0}^{n} \frac{3^\omega \binom{n}{\omega}}{4^n} \lambda_\omega. \tag{5.19}$$

The problem of measuring the average fidelity has been translated into the problem of measuring the eigenvalues $\{\lambda_\omega\}$ of the twirled channel $\bar{\Lambda}_{\mathcal{C}_1\Pi}$. How can this be achieved? If we would have access to the twirled channel $\bar{\Lambda}_{\mathcal{C}_1\Pi}$, then we could measure the eigenvalues by doing n different experiments, each using one of the following n input state's deviations

$$\rho_\omega = Z^{\otimes\omega} I^{\otimes n-\omega}, \;\; \omega \in \{1, \ldots, n\}. \tag{5.20}$$

In each experiment, we would send the input state through the averaged channel and then measure its expectation value, *i.e.* its projection onto itself, to get the corresponding eigenvalue. Obviously we do not actually have access the averaged channel, rather we only have access to the original channel Λ. Let's look at the expression of a specific λ_ω, and let $\mathrm{wt}(P) = \omega$. Remembering that the definition of $\bar{\Lambda}_{\mathcal{C}_1\Pi}$ is given by Eq.(5.12), it follows that

$$\begin{aligned}
\lambda_\omega = \frac{1}{2^n}\mathrm{tr}\left(P\bar{\Lambda}_{\mathcal{C}_1\Pi}(P)\right) &= \frac{1}{2^n|\mathcal{C}_1\Pi|} \sum_{v_i \in \mathcal{C}_1\Pi} \mathrm{tr}\left(P{v_i}^\dagger \Lambda(v_i P {v_i}^\dagger) v_i\right) \\
&= \frac{1}{2^n|\mathcal{C}_1\Pi|} \sum_{v_i \in \mathcal{C}_1\Pi} \mathrm{tr}\left(\Lambda(v_i P {v_i}^\dagger) v_i P {v_i}^\dagger\right) \\
&= \frac{1}{2^n 3^\omega \binom{n}{\omega}} \sum_{\mathrm{wt}(P_i \in \mathcal{P}_n)=\omega} \mathrm{tr}\left(\Lambda(P_i)P_i\right).
\end{aligned} \tag{5.21}$$

where the last line follows from the fact that there are only $3^\omega\binom{n}{\omega}$ different values of $P_i = v_i P {v_i}^\dagger$ for $v_i \in \mathcal{C}_1\Pi$. We see that λ_ω is the average of a uniformly distributed random variable T_ω that can take any of the $3^\omega\binom{n}{\omega}$ values in the set

$$\mathcal{T}_\omega = \{t_i \mid t_i = \tfrac{1}{2^n}\mathrm{tr}\left(\Lambda(P_i)P_i\right),\; P_i \in \mathcal{P}_n,\; \mathrm{wt}(P_i) = \omega\}. \tag{5.22}$$

The problem of measuring λ_ω has been translated into the problem of measuring the elements of $\mathcal{T}_\omega$. We now present the experimental procedure to achieve this. Let's consider an n-qubit system, and assume that the available initial states are those in the set

$$\mathcal{D} = \{\pi_k Z^{\otimes\omega} I^{\otimes n-\omega} \pi_k{}^\dagger |\ \omega \in \{1,\ldots,n\},\ \pi_k \in \Pi_n\}, \tag{5.23}$$

where Π_n is the group of permutation of n qubits. In other words, we can start the experiment with any state in the set $\mathcal{D}$. In addition, we will assume that only single-spin $\pi/2$ rotations are available. Now, let's say that we want to measure $t_i = \frac{1}{2^n}\mathrm{tr}\,(\Lambda(P_i)P_i)$, where $P_i \in \mathcal{P}_n$ and $\mathrm{wt}(P_i) = \omega$. We proceed as follows: we start with the operator $P \in \mathcal{D}$ that has weight ω and that has its identity terms at the same positions than the identity terms of P_i. For example, if $P_i = XIIY$, then we would start with $P = ZIIZ$. Next, we find the sequence of single-spin $\pi/2$ rotations, here we denote this sequence by v_i, such that $P_i = v_i P v_i{}^\dagger$. Finally, we measure the expectation value of P_i. The circuit summarizing this protocol is illustrated below in Figure 5.1

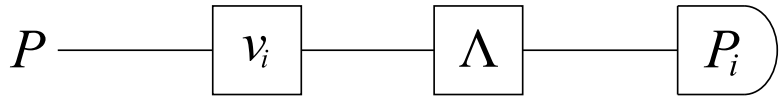

Figure 5.1: Circuit to measure $t_i = \frac{1}{2^n}\mathrm{tr}\,(\Lambda(P_i)P_i)$, where $P_i \in \mathcal{P}_n$ such that $\mathrm{wt}(P_i) = \omega$. Here, $P \in \mathcal{D}$ has weight ω and, in the tensor product form, its identity terms are at the same positions than the identity terms of P_i. The operator v_i represents a sequence of single-spin $\pi/2$ such that $P_i = v_i P v_i{}^\dagger$.

In the scheme presented above, it is implied that Λ is the error associated to an experimental implementation of the identity gate. However, as it is shown in [58], this scheme can be extended to the case for which the gate to be certified is an element of the Clifford group. This can easily be understood. Let Λ be the error associated to some unitary gate $\mathcal{U}$, and let's assume that we only have access to the imperfect implementation of $\mathcal{U}$. For the following scheme to work, we will see that $\mathcal{U}$ has to be an element of the Clifford group, and that its imperfect implementation can be written in the form $\tilde{\mathcal{U}} = \Lambda \circ \mathcal{U}$. Then, by inserting the identity gate as $\mathcal{U}^\dagger \circ \mathcal{U}$ in the circuit of Figure 5.1, it can be seen that this circuit can be written as in Figure 5.2.

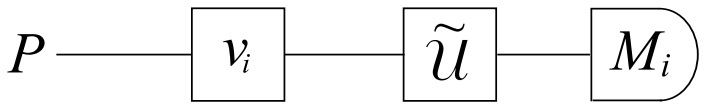

Figure 5.2: Modification of the circuit of Figure 5.1 by inserting the identity gate as $\mathcal{U}^\dagger \circ \mathcal{U}$, where $\mathcal{U}$ is a Clifford and $\tilde{\mathcal{U}} = \Lambda \circ \mathcal{U}$ is its faulty implementation. The measurement $M_i = \mathcal{U}(P_i)$ is also a Pauli operator. This circuit is equivalent to that of Figure 5.1.

In the context of NMR implementations, the circuit of Figure 5.2 needs to be slightly modified in order to account for the fact that we can't measure operators that do not correspond to (-1)-coherences. In other words, it won't always be possible to directly perform the measurement in Figure 5.2. However, there is a workaround using *readout pulses*. Let's say that a Pauli operator M_i can't be directly observed. Then, we can still apply a readout pulse R and then measure a different operator $O_i = RM_iR^\dagger$, where R is chosen so that O_i can be observed in a NMR experiment. Due to the fact that M_i is a Pauli operator, single-spin $\pi/2$ rotations are sufficient to map M_i to another Pauli operator that can be observed. Thus, R is a sequence of single-spin $\pi/2$ rotations and O_i is a Pauli operator. The above explanation is summarized in Figure 5.3

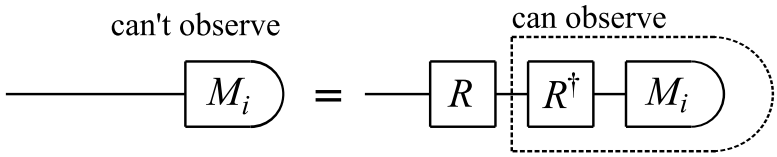

Figure 5.3: Here, $M_i \in \mathcal{P}_n$ is an operator that can't be observed directly in an NMR experiment. However, we can find a sequence R of single-spin $\pi/2$ rotations so that the Pauli operator $O_i = RM_iR^\dagger$ can be directly observed in an NMR experiment.

To account for this experimental constraint, we have to modify the circuit of Figure 5.2. The corrected circuit uses readout pulses and is illustrated in Figure 5.4.

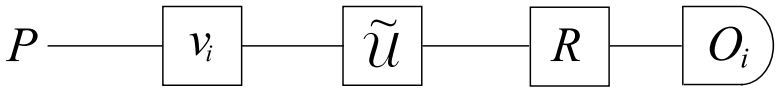

Figure 5.4: Modification of the circuit of Figure 5.2 using a readout pulse R consisting of single-spin $\pi/2$ rotations, and such that the Pauli operator $O_i = RM_iR^\dagger$ can be directly measured in the context of an NMR implementation.

Thus, by repeating the experiment of Figure 5.4 with different v_i, we can measure each of the elements of the set $\mathcal{T}_\omega$, and thus estimate the eigenvalue λ_ω. Repeating this procedure for all eigenvalues, we can then calculate the probability of no error with Eq.(5.19). Given that $\Pr(0) = [\chi]_{00}$, we can then calculate the average fidelity using Eq.(5.11).

In this section, we have presented a twirling protocol to estimate the average fidelity of Clifford gates. Although in practice we only have access to noisy measurements, repetitions can be used to decrease the noise. Therefore, in the following sections we won't consider the presence of noise in the measurements. How many elements of $\mathcal{T}_\omega$ do we need to measure in order to estimate λ_ω to some desired accuracy? Two approaches will be explored in order to answer this question. The first one uses an analytical result known as the Hoeffding's inequality. The second approach uses Monte Carlo simulations.

5.3 Statistical analysis

In the previous section, we have shown that the average fidelity of Clifford gates can be estimated by measuring the eigenvalues of the $\mathcal{C}_1\Pi$ twirled channel. We also showed that each of these eigenvalues can be written down as the statistical mean of a set of measured expectation values. In principle, measuring all of these expectation values is unnecessary if one only desires to approximate the mean. How many of these expectation values do we need to measure in order to reach a desired accuracy? This is the question addressed in the section. We will follow the work of J. Emerson et al. [59] and use two known results in probability and statistics: the Hoeffding's inequality, and the union bound.

The *Hoeffding's inequality* [60] is a general result in probability and statistics that we are going to use in this section. It states that if $x_1, \ldots, x_N$ are independent realizations of a random variable X, confined to the interval $[a, b]$ and with statistical mean $\mathbb{E}(X) = \mu$, then for any $\delta > 0$ we have

$$\Pr(|\bar{X} - \mu| > \delta) \leq 2e^{-2\delta^2 N/(b-a)^2}, \tag{5.24}$$

where $\bar{X} = \frac{1}{N}\sum_{i=1}^{N} x_i$ is the estimator of the exact mean μ, and where $\Pr(\mathcal{E})$ denotes the probability of event $\mathcal{E}$. In other words, the Hoeffding's inequality provides an upper bound to the probability that the estimated mean is off by a value greater than δ.

We now apply Hoeffding's inequality to the random variable T_ω, which was defined in the previous section as a uniformly distributed random variable that can take any of the $3^\omega\binom{n}{\omega}$ values in the set

$$\mathcal{T}_\omega = \{t_i \mid t_i = \tfrac{1}{2^n}\mathrm{tr}\left(\Lambda(P_i)P_i\right),\ P_i \in \mathcal{P}_n,\ \mathrm{wt}(P_i) = \omega\}.$$

We see that T_ω is bounded to the interval $[-1, 1]$. Our goal to estimated the mean $\mathbb{E}(T_\omega) = \lambda_\omega$. Let $t_1, \ldots, t_{k_\omega}$ be independent realizations of T_ω. The estimator of λ_ω is hence $\tilde{\lambda}_\omega = \frac{1}{k_\omega}\sum_{i=1}^{k_\omega} t_i$, and from Hoeffding's inequality it follows that for any $\delta > 0$,

$$\Pr_{\mathcal{E}_\omega} := \Pr\left(|\tilde{\lambda}_\omega - \lambda_\omega| > \delta\right) \leq 2e^{-\delta^2 k_\omega/2}. \tag{5.25}$$

By taking the natural logarithm of each side of this inequality, we see that the number of realizations required to estimate λ_ω to precision δ with constant probability obeys

$$k_\omega \leq \frac{2\ln(2/\Pr_{\mathcal{E}_\omega})}{\delta^2}. \tag{5.26}$$

This upper bound is sufficient if we want to estimate a single eigenvalue λ_ω. We next use the union bound to extend this result to the estimation of the complete set $\{\lambda_1, \ldots, \lambda_n\}$.

The *union bound* [60] is a general result in probability and statistics that applies for an arbitrary set of possible events $\{\mathcal{E}_1, \ldots, \mathcal{E}_n\}$. Let $\Pr_{\mathcal{E}_\omega}$ denote the probability that event $\mathcal{E}_\omega$ happens, and let $\Pr_{\vee\mathcal{E}_\omega}$ denote the probability that at least one of the possible events happens. Then, the union bound states that

$$\Pr_{\vee\mathcal{E}_\omega} \leq \sum_{\omega=1}^{n} \Pr_{\mathcal{E}_\omega}. \tag{5.27}$$

We now apply this result to our particular problem, in which case $\mathcal{E}_\omega$ denotes the event $|\tilde{\lambda}_\omega - \lambda_\omega| > \delta$. In other words, $\mathcal{E}_\omega$ is the event that $\tilde{\lambda}_\omega$ is outside of the precision δ. Similarly, $\vee\mathcal{E}_\omega$ denotes the event that at least one element of $\{\tilde{\lambda}_1, \ldots, \tilde{\lambda}_n\}$ is outside of the precision δ. Applying the union bound and using Eq.(5.25), it follows that

$$\Pr_{\vee\mathcal{E}_\omega} \leq 2 \sum_{\omega=1}^{n} e^{-\delta^2 k_\omega/2}. \tag{5.28}$$

If we make the assumption that $k_1 = k_2 = \cdots = k_n$, then it follows that

$$\Pr_{\vee\mathcal{E}_\omega} \leq 2n\, e^{-\delta^2 k_\omega/2}. \tag{5.29}$$

Then again, taking the natural logarithm of each side, we find that

$$k_\omega \leq \frac{2\ln(2n/\Pr_{\vee\mathcal{E}_\omega})}{\delta^2}. \tag{5.30}$$

The previous result is an upper bound to the number of independent realizations that are required for estimating each element of the set $\{\lambda_1, \ldots, \lambda_n\}$ to precision within δ with constant probability. We now discuss the practical limitations of this result.

The problem with the approach presented in this section is that it is useful only when n is large enough. This is due to the fact that this approach works for any random variable confined to $[-1, 1]$, *i.e.* the approach is very general. For our particular problem, the set $\mathcal{T}_\omega$ has $3^\omega \binom{n}{\omega}$ elements. Therefore, if the upper bound on k_ω is bigger than

$$K_\omega = 3^\omega \binom{n}{\omega}, \tag{5.31}$$

then the results obtained in this section are useless from a practical point of view.

In this section, we have shown how Hoeffding's inequality and the union bound can be used to derive an upper bound on the number of measurements required to estimate the eigenvalues of a twirled channel. We have also shown that this upper bound is an asymptotical result that is useful only when the number of qubits n is large enough. In the next section, we will explore an alternate approach based on Monte Carlo simulations.

5.4 Monte Carlo simulations

We have seen that the average fidelity of a quantum channel Λ can be obtained from the eigenvalues $\{\lambda_0, \ldots, \lambda_n\}$ of its twirled channel $\bar{\Lambda}_{\mathcal{C}_1\Pi}$. By default we have $\lambda_0 = 1$, but we still need to measure the n remaining eigenvalues. In this section we explore how Monte Carlo simulations can help us understand how many measurements we need to do to approximate these eigenvalues. We explore two noisy channel models and study their statistical properties numerically and analytically. We show that there is a relation between the number of measurements required and the spread in the elements of the χ matrix of the channel. Using this relation, we numerically study worst case scenarios.

Let's first remind us of the problem that we are interested to solve here. As we have see in section 5.2, the eigenvalues of the twirled channel $\bar{\Lambda}_{\mathcal{C}_1\Pi}$ can be written as

$$\lambda_\omega = \frac{1}{3^\omega \binom{n}{\omega}} \sum_{\mathrm{wt}(P_i \in \mathcal{P}_n)=\omega} t_i, \qquad \text{where } \; t_i = \tfrac{1}{2^n} \mathrm{tr}\left(\Lambda(P_i) P_i\right).$$

The terms $\{t_i\}$ can be measured experimentally, but measuring all of them is unnecessary if one only desires to obtain a reasonable approximation. How many of these t_i do we need to measure in order to get a good estimate of λ_ω? In the previous section, we saw that Hoeffding's inequality can be applied to this problem, but only to derive an asymptotical result that is useful when the number n of qubits is large enough. Here, we study an alternate approach, based on *Monte Carlo simulations*, that aims to estimate the standard error in the estimator of λ_ω as a function of the number of measurements.

Let us first discuss the notation that we will use in the rest of this section. As the reader already knowns, in probability theory, the average, the variance and the standard deviation of a random variable X are usually denoted respectively by $\mathbb{E}[X]$, $\mathrm{Var}(X)$ and $\mathrm{Std}(X)$. Here, we will extend this notation to deterministic sets and vectors. Let $S = \{s_1, s_2, \ldots, s_N\}$ be a set with deterministic elements, and let $\boldsymbol{v} = (v_1, v_2, \ldots, v_M)^\top$ be a vector with deterministic components. Then, we have the following notation rules

$$\begin{aligned}
\mathbb{E}_S[S] &= \frac{1}{N}\sum_{i=1}^{N} s_i, & \mathbb{E}_V[\boldsymbol{v}] &= \frac{1}{M}\sum_{i=1}^{M} v_i, \\
\mathrm{Var}_S(S) &= \frac{1}{N}\sum_{i=1}^{N} s_i^2 - \mathbb{E}_S[S]^2, & \mathrm{Var}_V(\boldsymbol{v}) &= \frac{1}{M}\sum_{i=1}^{M} v_i^2 - \mathbb{E}_V[\boldsymbol{v}]^2, \\
\mathrm{Std}_S(S) &= \sqrt{\mathrm{Var}_S(S)}, & \mathrm{Std}_V(\boldsymbol{v}) &= \sqrt{\mathrm{Var}_V(\boldsymbol{v})}.
\end{aligned}$$

The reason for this notation is that we will often store the possible outcomes of uniformly distributed random variables into sets or vectors. Thus, this notation provides a shortcut when we want to denote statistical properties of such random variables.

We now return to the problem of estimating an eigenvalue λ_ω of the twirled channel. The set of all possible measurements for a given λ_ω is

$$\mathcal{T}_\omega = \{t_i \mid t_i = \tfrac{1}{2^n}\mathrm{tr}\left(\Lambda(P_i)P_i\right),\ P_i \in \mathcal{P}_n,\ \mathrm{wt}(P_i) = \omega\}.$$

In section 5.2, we have shown that $\mathbb{E}_S[T_\omega] = \lambda_\omega$. Now let's choose at random k_ω different elements of this set. In other words, we choose a random subset $\mathcal{I} \subset \mathcal{T}_\omega$ such that $|\mathcal{I}| = k_\omega$. The average value $\mathbb{E}_S[\mathcal{I}]$ of this subset is a realization of the *estimator* of λ_ω. The estimator of λ_ω is denoted $\tilde{\lambda}_\omega$ and is itself a random variable, meaning that if we repeat the process of choosing a random subset of $\mathcal{T}_\omega$ and take its average value, then for k_ω small enough we will most likely get a different value than the one previously obtained. Obviously, we have $\mathbb{E}[\tilde{\lambda}_\omega] = \lambda_\omega$ for any value of k_ω, and here we are interested in the uncertainty in the estimator as a function of k_ω. Specifically, we will study the standard deviation of $\tilde{\lambda}_\omega$ as a function of k_ω. Of course, without the ability to make educated assumptions about the specific quantum channel to be certified, the best we can do is to study a large number of randomly chosen channels. Here, we will consider Pauli channels with average fidelity $\bar{F} \in [0.7, 1]$, and we will later show why this analysis should be sufficient. In the following, we describe a first approach to generate such random Pauli channels.

Many algorithms for generating quantum channels could have been explored, and many types of channels with different properties could have been studied. The goal here is to show how the general procedure works, and propose models that are relevant. In the following, we present one way of generating random Pauli channels with desired average fidelity. The first step in generating a random Pauli channel is to choose uniformly at random its average fidelity $\bar{F}$ in the interval $[0.7, 1]$, and then calculate the probability of no error as $\Pr(0) = \frac{(2^n+1)\bar{F}-1}{2^n}$. Next, we choose the other probabilities $\{\Pr(1), \ldots, \Pr(n)\}$ uniformly at random in the interval $[0, 1]$, and then divide them by a same constant such that they sum up to $1 - \Pr(0)$. Then, we have to generate the elements of the χ matrix, which is a diagonal matrix since we consider Pauli channels. We have already shown that the relationship between the elements of χ and the probabilities of errors is given by

$$\Pr(\omega) = \sum_{\mathrm{wt}(P_i \in \mathcal{P}_n) = \omega} [\chi]_{ii}.$$

In particular, this implies that $[\chi]_{00} = \Pr(0)$. The strategy to choose the remaining entries of χ is again to generate random sets with elements in $[0, 1]$ and then normalize them so that they sum up to their corresponding $\Pr(\omega)$. In summary, the idea is to start from the average fidelity of the channel, then choose randomly the elements of $\{\Pr(1), \ldots, \Pr(n)\}$, and finally choose randomly the entries of the χ matrix. This method for generating random Pauli channels is summarized in the pseudo-code below.

Choose $\bar{F}$ uniformly at random in $[0.7, 1]$

Compute $\Pr(0) = \frac{(2^n+1)\bar{F}-1}{2^n}$

Choose the elements of $\{\Pr(\omega)|\omega = 1, \ldots, n\}$ uniformly at random in [0, 1]

Divide them by a same constant s.t. $\sum_{\omega=1}^{n} \Pr(\omega) = 1 - \Pr(0)$

for $\omega = 0 : n$ **do**

  Choose the $\{[\chi]_{ii} \mid \mathrm{wt}(P_i \in \mathcal{P}_n) = \omega\}$ uniformly at random in $[0, 1]$

  Divide them by a same constant s.t. $\sum_{\mathrm{wt}(P_i \in \mathcal{P}_n)=\omega} [\chi]_{ii} = \Pr(\omega)$

end

Algorithm 3: Pseudo-code to generate a random Pauli channel with $0.7 \leq \bar{F} \leq 1$.

We now describe how we study the standard deviation of the estimator $\tilde{\lambda}_\omega$ as a function of the number of measurements k_ω. The first step is to generate a random Pauli channel using the algorithm described above. Then, for each value of $\omega \in \{1, \ldots, n\}$, we compute the standard deviation of the estimator $\tilde{\lambda}_\omega$ for each value of $k_\omega \in \{1, \ldots, 3^\omega \binom{n}{\omega}\}$. We repeat the whole process a large number of times and we average over a sufficiently large number of random Pauli channels. The details of the algorithm are summarized in the pseudo-code below. The output is the standard deviation of the estimator $\tilde{\lambda}_\omega$ as a function of the number of measurements k_ω. The standard deviation is averaged over a large number of random Pauli channels, and is thus denoted $\overline{\mathrm{Std}}$.

Generate a random Pauli channel Λ

for $\omega = 1 : n$ **do**

  Compute the set $\mathcal{T}_\omega = \{t_i \mid t_i = \frac{1}{2^n}\mathrm{tr}\left(\Lambda(P_i)P_i\right),\ P_i \in \mathcal{P}_n,\ \mathrm{wt}(P_i) = \omega\}$

  for $k_\omega = 1 : 3^\omega \binom{n}{\omega}$ **do**

    for $j = 1 : N$ **do**

      Choose a subset $\mathcal{I} \subset \mathcal{T}_\omega$ at random and s.t. $|\mathcal{I}| = k_\omega$

      Compute $\mathbb{E}_S[\mathcal{I}]$ and store this value at position j in vector $\tilde{\boldsymbol{\lambda}}_\omega$

    end

    Compute $\mathrm{Std}_V(\tilde{\boldsymbol{\lambda}}_\omega)$ and store this value at position k_ω in vector $\mathbf{std}_\omega$

  end

end

Repeat a large number of times and average over all random Pauli channels

Algorithm 4: Monte Carlo algorithm for estimating the standard deviation of the estimator $\tilde{\lambda}_\omega$ as a function of the number of measurements k_ω. Here, N is a number sufficiently large. The standard deviation is averaged over a large number of channels.

We performed this Monte Carlo simulation considering $n = 4$ qubits and taking the average over 300 random Pauli channels. The results are given in Figure. 5.5. We see that the standard deviation is quite small even for small values of k_ω. This is intuitively due to the variance in the elements of the χ matrix. In fact, we can show that there is a relationship between the variance of χ and the variance of $\mathcal{T}_\omega$.

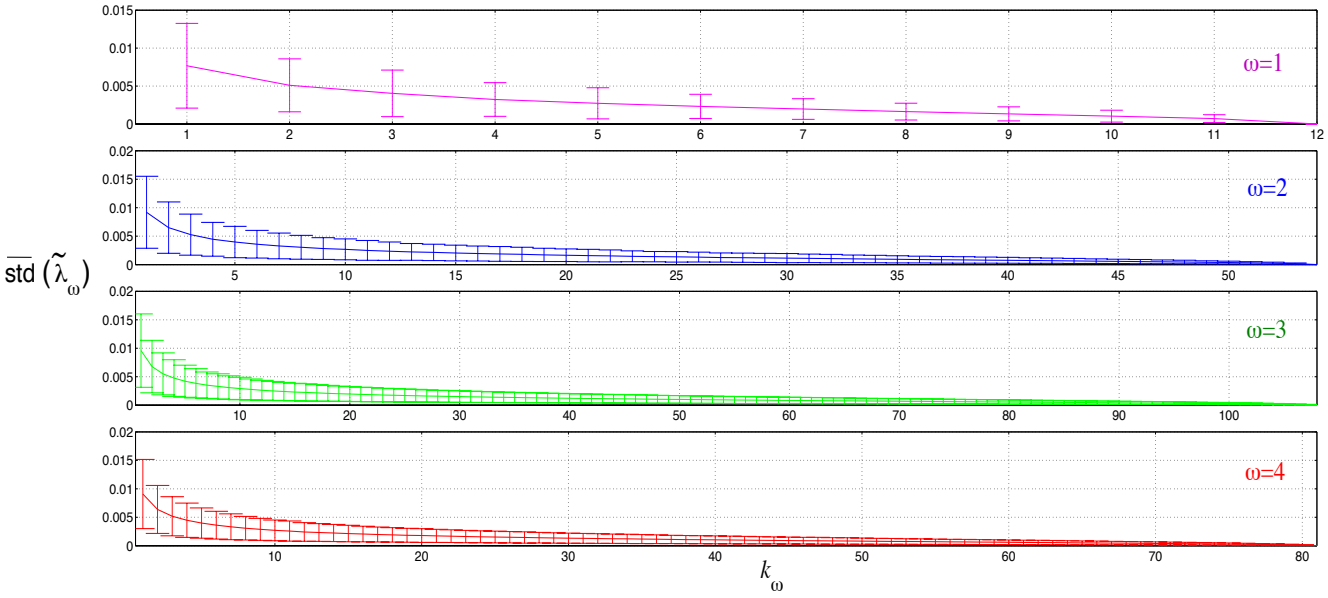

Figure 5.5: Results of the Monte Carlo simulations for $n = 4$. Each graph corresponds to a specific value of ω. The y-axis is the average standard deviation of the estimator $\tilde{\lambda}_\omega$, and the x-axis is the value of k_ω. The average is taken over 300 random Pauli channels with $0.7 \leq \bar{F} \leq 1$. Note that the standard error is very low even for small k_ω.

We now derive the relationship between the variance in the elements of the χ matrix and the variance in the elements of $\mathcal{T}_\omega = \{t_i \mid t_i = \frac{1}{2^n}\mathrm{tr}\left(\Lambda(P_i)P_i\right),\ P_i \in \mathcal{P}_n,\ \mathrm{wt}(P_i) = \omega\}$. For a general channel Λ, we have that

$$\Lambda(P_i) = \sum_{P_j, P_k \in \mathcal{P}_n} [\chi]_{jk} P_j P_i P_k = \sum_{P_j, P_k \in \mathcal{P}_n} (-1)^{c_{ik}} [\chi]_{jk} P_j P_k P_i, \tag{5.32}$$

where

$$c_{ik} = \begin{cases} 0 & \text{if } P_i \text{ and } P_k \text{ commute} \\ 1 & \text{if } P_i \text{ and } P_k \text{ anti-commute.} \end{cases} \tag{5.33}$$

This is due to the fact that Pauli operators either commute or anti-commute with each others. From this, it follows that we can write down t_i as

$$\begin{aligned} t_i &= \tfrac{1}{2^n}\mathrm{tr}\left(\Lambda(P_i)P_i\right) \\ &= \sum_{P_j \in \mathcal{P}_n} (-1)^{c_{ij}} [\chi]_{jj}. \end{aligned} \tag{5.34}$$

Taking the variance of the set $\mathcal{T}_\omega$, as described at the beginning of this section, we obtain

$$\mathrm{Var}_S(\mathcal{T}_\omega) = \frac{1}{3^\omega \binom{n}{\omega}} \left(\sum_{\mathrm{wt}(P_i \in \mathcal{P}_n) = \omega} {t_i}^2 \right) - {\lambda_\omega}^2. \tag{5.35}$$

From the above equation, it seems that we should be looking for an expression for ${t_i}^2$. From Eq.(5.34), we obviously have that

$$\begin{aligned} {t_i}^2 &= \left(\sum_{P_j \in \mathcal{P}_n} (-1)^{c_{ij}} [\chi]_{jj} \right) \left(\sum_{P_k \in \mathcal{P}_n} (-1)^{c_{ik}} [\chi]_{kk} \right) \\ &= \sum_{P_j, P_k \in \mathcal{P}_n} (-1)^{c_{ij}+c_{ik}} [\chi]_{jj} [\chi]_{kk} \\ &= \sum_{P_j \in \mathcal{P}_n} {[\chi]_{jj}}^2 + \sum_{\substack{P_j, P_k \in \mathcal{P}_n \\ (P_j \neq P_k)}} (-1)^{c_{ij}+c_{ik}} [\chi]_{jj} [\chi]_{kk}. \end{aligned} \tag{5.36}$$

Therefore, it follows that

$$\begin{aligned} \sum_{\mathrm{wt}(P_i \in \mathcal{P}_n) = \omega} {t_i}^2 &= \sum_{\mathrm{wt}(P_i \in \mathcal{P}_n) = \omega} \left(\sum_{P_j \in \mathcal{P}_n} {[\chi]_{jj}}^2 + \sum_{\substack{P_j, P_k \in \mathcal{P}_n \\ (P_j \neq P_k)}} (-1)^{c_{ij}+c_{ik}} [\chi]_{jj} [\chi]_{kk} \right) \\ &= 3^\omega \binom{n}{\omega} \sum_{P_j \in \mathcal{P}_n} {[\chi]_{jj}}^2 + \sum_{\mathrm{wt}(P_i \in \mathcal{P}_n) = \omega} \left(\sum_{\substack{P_j, P_k \in \mathcal{P}_n \\ (P_j \neq P_k)}} (-1)^{c_{ij}+c_{ik}} [\chi]_{jj} [\chi]_{kk} \right) \\ &\approx 3^\omega \binom{n}{\omega} \sum_{P_j \in \mathcal{P}_n} {[\chi]_{jj}}^2, \end{aligned} \tag{5.37}$$

where the last line follows from the fact that the second term is very small (typically less than 2% of the full value), and can thus be neglected to a very good approximation. From Eq.(5.35), it follows that the variance in the elements of $\mathcal{T}_\omega$ is given by

$$\mathrm{Var}_S(\mathcal{T}_\omega) \approx \left(\sum_{P_j \in \mathcal{P}_n} {[\chi]_{jj}}^2 \right) - {\lambda_\omega}^2. \tag{5.38}$$

Now, let $\boldsymbol{\chi}_{diag}$ denote the vector containing the diagonal entries of the χ matrix. Given that χ has dimensions $4^n \times 4^n$ and that $\mathrm{tr}(\chi) = 1$, it follows that the variance of $\boldsymbol{\chi}_{diag}$ is

$$\mathrm{Var}_V(\boldsymbol{\chi}_{diag}) = \frac{1}{4^n} \left(\sum_{P_j \in \mathcal{P}_n} {[\chi]_{jj}}^2 \right) - \left(\frac{1}{4^n} \right)^2. \tag{5.39}$$

We see that for a fixed value of λ_ω, the variance of $\mathcal{T}_\omega$ increases as the variance in the diagonal entries of χ increases. For a given set of probabilities $\{\Pr(\omega)\}$, the variance of $\mathcal{T}_\omega$ is therefore maximized by choosing the matrix χ such that its diagonal entries have maximal variance. This is done by choosing that only $n+1$ entries of the diagonal of χ are non zero with value equal to one of the elements of $\{\Pr(\omega)\}$. We can now start to think about studying some kind of worst case scenario. Namely, we will still consider random Pauli channels with $0.7 \leq \bar{F} \leq 1$, but the elements of the χ matrix will now be chosen randomly with the constraint that they must maximize the variance of their distribution. According to our proof, this ensures that the elements of $\mathcal{T}_\omega$ will also have a maximized variance. Moreover, as we have shown above, for a fixed λ_ω we have that $\mathrm{Var}(\mathcal{T}_\omega)$ depends mainly on the variance in the diagonal entries of the χ matrix. This implies that considering Pauli channels is sufficient. Hence, the Monte Carlo simulation will effectively correspond to a worst case scenario, even if we only consider Pauli channels. This method to generate random Pauli channels is summarized in the pseudo-code below.

1 Choose $\bar{F}$ uniformly at random in $[0.7, 1]$

2 Compute $\Pr(0) = \frac{(2^n+1)\bar{F}-1}{2^n}$

3 Choose the elements of $\{\Pr(\omega)|\omega = 1, \ldots, n\}$ uniformly at random in [0, 1]

4 Divide them by a same constant s.t. $\sum_{\omega=1}^{n} \Pr(\omega) = 1 - \Pr(0)$

5 **for** $\omega = 0 : n$ **do**

  Set i by randomly picking one element of the set $\{i \mid \mathrm{wt}\,(P_i \in \mathcal{P}_n) = \omega\}$

  Set $[\chi]_{ii} = \Pr(\omega)$

end

Algorithm 5: Pseudo-code to generate a random Pauli channel with $0.7 \leq \bar{F} \leq 1$ and maximized variance. Only $n+1$ entries of χ are non zero.

We perform the Monte Carlo simulations again, but now using the above algorithm to generate the random Pauli channels, so as to maximize the variance of the estimator $\tilde{\lambda}_\omega$. Again, we choose the same threshold for the average fidelity and we average over 300 random Pauli channels. The results for $n = 4$ qubits are given in Figure 5.6. Although the standard error is increased roughly an order of magnitude with respect to the previous simulations, only half of the total number of measurements seems to be required in order to have an average standard error less than 0.02. Thus, doing half of the experiments should be enough to have at least this kind of statistical accuracy, since this analysis with Pauli channels can be applied to our particular channel to be certified in experiment as we have demonstrated above. In fact, the standard error can be used as the error bar since $\tilde{\lambda}_\omega$ is Gaussian distributed, as it can be observed from Figure 5.7.

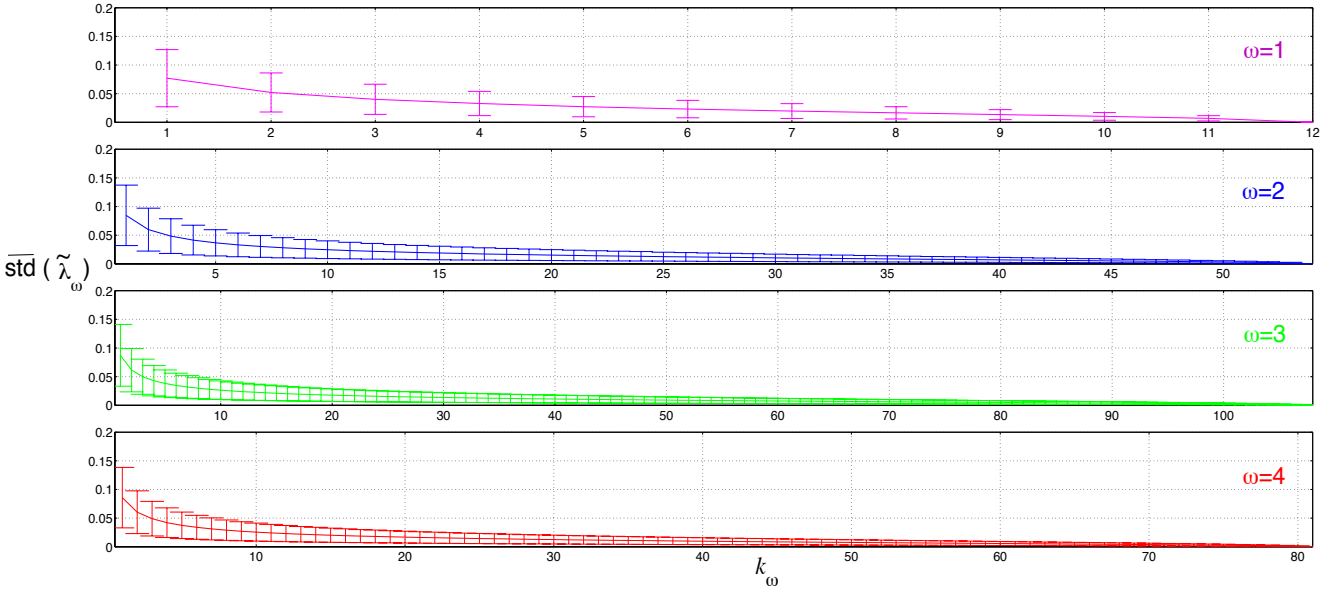

Figure 5.6: Results of the "worst case" Monte Carlo simulations for $n = 4$. Each graph corresponds to a specific ω. The y-axis is the average standard deviation of the estimator $\tilde{\lambda}_\omega$, and the x-axis is the value of k_ω. The average is taken over 300 random Pauli channels with $0.7 \leq \bar{F} \leq 1$ and such that the elements of χ have maximal variance. The standard error is increased roughly by an order of magnitude compared to the previous simulation.

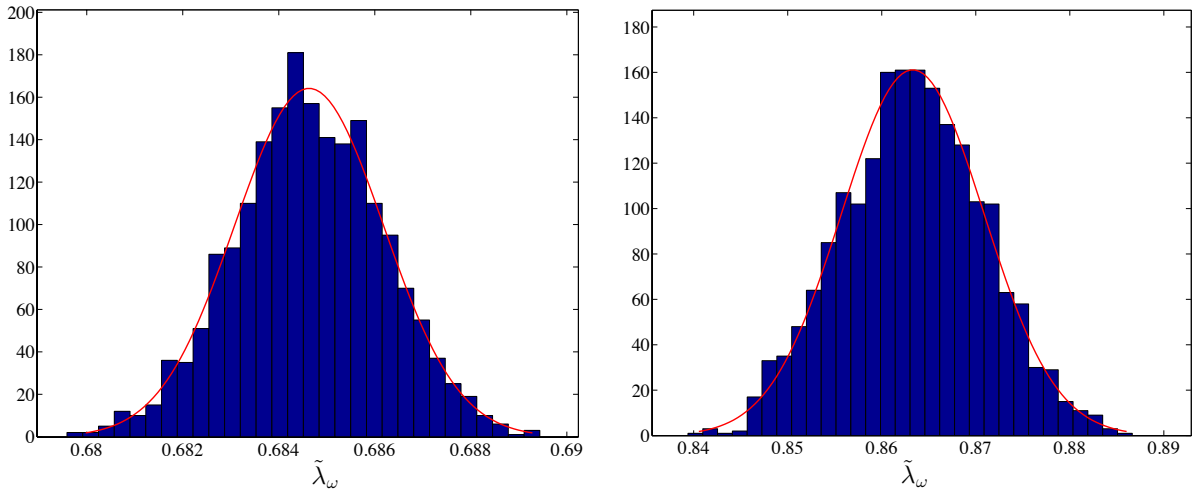

Figure 5.7: Histogram for the distribution of the estimator $\tilde{\lambda}_\omega$ for a 4-qubit random Pauli channel, fitted to a Gaussian distribution. The parameters are $k_\omega = 50$ and $\omega = 3$. The random Pauli channel is generated using **(Left)** Algorithm 3, and **(Right)** Algorithm 5.

The histograms displayed in Figure 5.7 give the frequency distribution of the estimator $\tilde{\lambda}_3$ with $k_3 = 50$ for some 4-qubit random Pauli channel. The results are given for a random channel generated using Algorithm 3, and also using Algorithm 5. The two distributions fit well to a Gaussian distribution. Therefore, we could use the confidence interval for Gaussian distributions as the statistical error bar for $\tilde{\lambda}_\omega$.

We now discuss an other important observation to be made from Eq.(5.38). In fact, it can be seen from this expression that the variance in the elements of $\mathcal{T}_\omega$ should be smaller for large values of λ_ω. From Eq.(5.16), it can be seen that we have

$$\lambda_\omega = \Pr(0) + \sum_{\omega'=1}^{n} [\Omega]_{\omega,\omega'} \Pr(\omega'), \quad \text{where } |[\Omega]_{\omega,\omega'}| \leq 1. \tag{5.40}$$

It thus follows that as the average fidelity approaches 1, $\Pr(\omega > 0)$ approaches 0 and λ_ω therefore approaches 1 as well. From Eq.(5.38) we conclude that as the average fidelity approaches 1, the variance in the elements of $\mathcal{T}_\omega$ approaches zero. From this observation, we conclude that for channels with an average fidelity that is expected to be high, less measurements should be required. In fact, we can prove and illustrate this point by deriving an upper bound for the variance in $\mathcal{T}_\omega$ as a function of the average fidelity.

First, let's derive a lower bound for λ_ω using Eq.(5.40). We can achieve this by letting $[\Omega]_{\omega,\omega'} = -1$, even though this is not actually true, it does allow us to derive a valid lower bound for λ_ω. Using the fact that $\sum_{\omega'=1}^{n} \Pr(\omega') = 1 - \Pr(0)$, we find that

$$\lambda_\omega \geq \Pr(0) - (1 - \Pr(0)) = 2\Pr(0) - 1 \tag{5.41}$$

Next, we focus on deriving an upper bound for the term $\sum_j [\chi]_{jj}{}^2$. Using the convention that $[\chi]_{00} = \Pr(0)$, it follows that the first term in the summation is $\Pr(0)^2$. One can easily understand that the case that maximizes $\sum_j [\chi]_{jj}{}^2$ is when there is only one other term that is nonzero. This term must then be equal to $(1 - \Pr(0))^2$. Thus, we conclude that a valid upper bound for $\sum_j [\chi]_{jj}{}^2$ is

$$\sum_j [\chi]_{jj}{}^2 \leq \Pr(0)^2 + (1 - \Pr(0))^2 = 2\Pr(0)^2 - 2\Pr(0) + 1. \tag{5.42}$$

We now have all the pieces that we need to formulate an upper bound for $\mathrm{Var}_S(\mathcal{T}_\omega)$. In fact, using Eq.(5.38) combined with the lower bound (5.41) and the upper bound (5.42), we find the following upper bound for $\mathrm{Var}_S(\mathcal{T}_\omega)$

$$\begin{aligned}
\mathrm{Var}_S(\mathcal{T}_\omega) &\leq (2\Pr(0)^2 - 2\Pr(0) + 1) - (2\Pr(0) - 1) \\
\Rightarrow \mathrm{Var}_S(\mathcal{T}_\omega) &\leq 2\Pr(0)^2 - 4\Pr(0) + 2 \\
\Rightarrow \mathrm{Var}_S(\mathcal{T}_\omega) &\leq 2(\Pr(0) - 1)^2 \\
\Rightarrow \mathrm{Std}_S(\mathcal{T}_\omega) &\leq \sqrt{2}|\Pr(0) - 1|.
\end{aligned} \tag{5.43}$$

Now, using the expression $\Pr(0) = \frac{(2^n+1)\bar{F}-1}{2^n}$, we can plot this upper bound as a function of $\bar{F}$, so as to verify if the standard deviation is bounded above by lower values as $\bar{F}$ increases. The results for $n = 3$, $n = 4$ and $n = 6$, are illustrated in Figure 5.8.

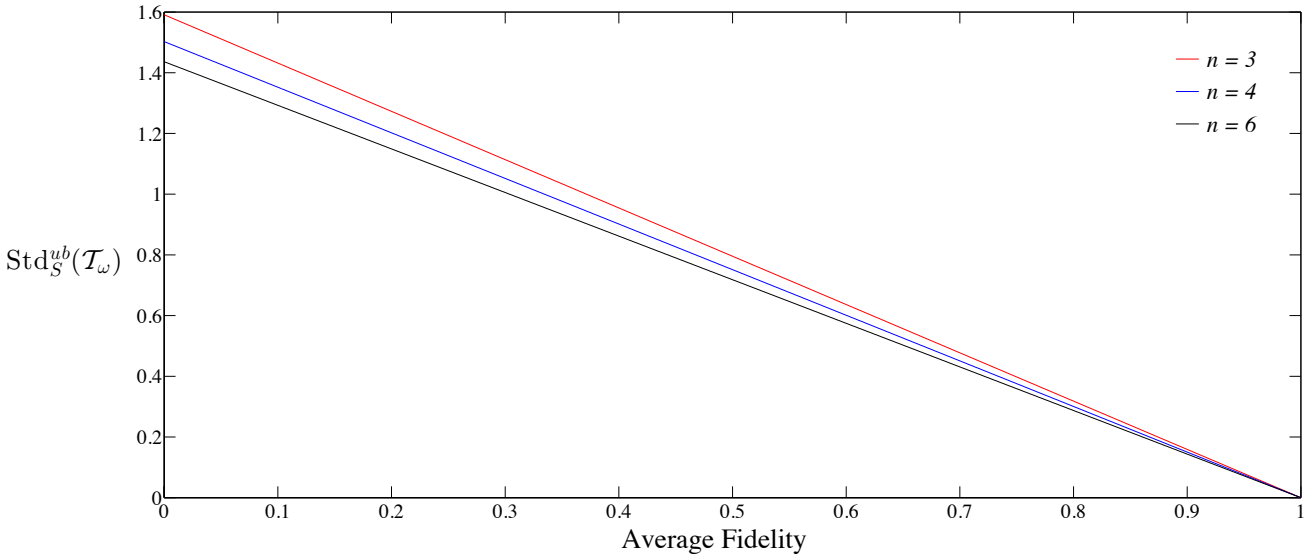

Figure 5.8: Upper bound for the standard deviation of $\mathcal{T}_\omega$ as a function of the average fidelity. We see that for $\bar{F} = 1$, the upper bound is at zero, which is a very sensible result. Thus, less experiments should be required for channels with expected high fidelities. As the average fidelity decreases, the upper bound increases following a straight line. The results are given for $n = 3$, $n = 4$ and $n = 6$ qubits.

The graph of Figure 5.8 illustrates perfectly that the standard deviation in the elements of $\mathcal{T}_\omega$ is bounded above by smaller values when the average fidelity is higher, demonstrating that in principle less experiments are required to reach the same statistical accuracy when the average fidelity of the channel is expected to be high. Now wether or not we do have access to this kind of information in reality is a different question.

In this section we have explored how Monte Carlo simulations can help us to estimate how many experiments we need to do in order to approximate the eigenvalues of a twirled channel $\bar{\Lambda}_{\mathcal{C}_1\Pi}$. We considered random Pauli channels with average fidelity $0.7 \leq \bar{F} \leq 1$, but other models could have been explored. The choice of these bounds for the average fidelity is justified by the assumption that the average fidelity of the channel to be certified is expected to be in that range. We derived an equation that shows how the variance in the elements of $\mathcal{T}_\omega$ is related to the variance in the diagonal entries of the χ matrix. We then used this relation to define a worst case Monte Carlo method, so as to get an idea of how many experiments we should do in the worst cases. The purpose of this chapter was to gain a better understanding of the relation between the χ matrix of the channel Λ to be certified, and the number of experiments that we should do to reach a desired accuracy. In practice, it is not necessary to known the number of experimental runs prior to start the experiment. As we perform the experimental runs we can monitor the variance in the data, and decides wether or not we need to do more experiments. In the next section, we will simulate the twirling certification experiment for a 4-qubit system.

5.6 Experimental results for a 2-qubit system

Calibration: The first certification experiment is more of a calibration procedure that aims to capture the errors in preparation and measurements. It is equivalent to certify the *do nothing* operation, which is a perfect implementation of the identity. The circuit for a generic experimental run is illustrated below, and the details are given in the table. In the table, the notation $(\pi/2)_k^u$ means that a $\pi/2$ rotation is applied to spin $k \in \{1, 2\}$ about the axis $u \in \{\pm x, \pm y, \pm z\}$.

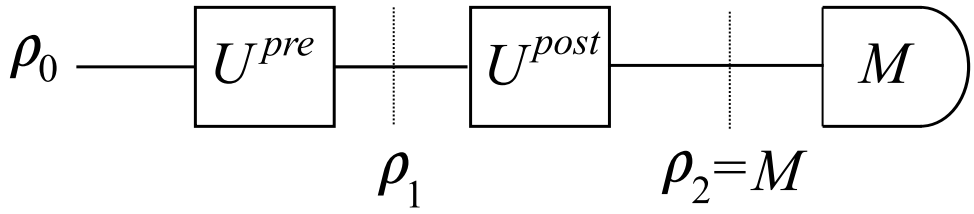

Figure 5.10: Circuit for a generic experimental run for the calibration step. The initial state is denoted ρ_0 and is mapped to some Pauli by the preparation operation U^{pre}. The readout pulse (if required) is denoted U^{post} and the measurement is denoted M. We choose that the measurement is equal to the state ρ_2, we thus have $\rho_2 = M$. The details for the specific values for each experiments are given in the table below.

Experiment #	ρ_0	U^{pre}	ρ_1	U^{post}	M
1	IZ	$(\pi/2)_2^y$	IX	–	IX
2	IZ	$(\pi/2)_2^{-x}$	IY	–	IY
3	IZ	–	IZ	$(\pi/2)_2^y$	IX
4	ZI	$(\pi/2)_1^y$	XI	–	XI
5	ZI	$(\pi/2)_1^{-x}$	YI	–	YI
6	ZI	–	ZI	$(\pi/2)_1^y$	XI
7	ZZ	$(\pi/2)_1^y(\pi/2)_2^y$	XX	$(\pi/2)_2^{-y}$	XZ
8	ZZ	$(\pi/2)_1^y(\pi/2)_2^{-x}$	XY	$(\pi/2)_2^x$	XZ
9	ZZ	$(\pi/2)_1^y$	XZ	–	XZ
10	ZZ	$(\pi/2)_1^{-x}(\pi/2)_2^y$	YX	$(\pi/2)_1^x$	ZX
11	ZZ	$(\pi/2)_1^{-x}(\pi/2)_2^{-x}$	YY	$(\pi/2)_1^x$	ZY
12	ZZ	$(\pi/2)_1^{-x}$	YZ	–	YZ
13	ZZ	$(\pi/2)_2^y$	ZX	–	ZX
14	ZZ	$(\pi/2)_2^{-x}$	ZY	–	ZY
15	ZZ	–	ZZ	$(\pi/2)_2^{-x}$	ZY

In practice, we also need to take reference spectra and label them so that we can remember which reference spectra should be used. In this experiment, the identity pulses

are implemented and have the same length as the other pulses.

CNOT: The other certification experiment to be done is with the CNOT gate. The circuit for a generic experimental run is illustrated bellow, and the details are given in the table that follows. Then again, in the table the notation $(\pi/2)_k^u$ means that a $\pi/2$ rotation is applied to spin $k \in \{1, 2\}$ about the axis $u \in \{\pm x, \pm y, \pm z\}$.

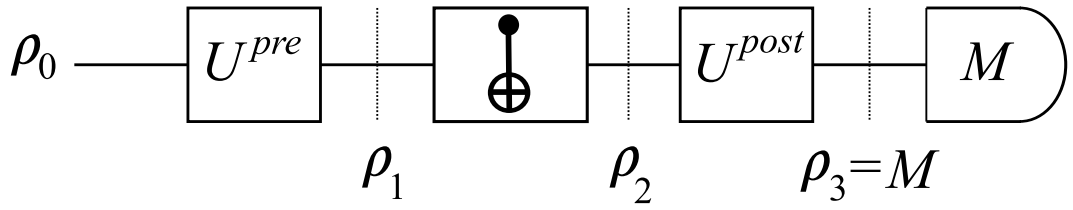

Figure 5.11: Circuit for a generic experimental run for certifying the CNOT gate. The initial state is denoted ρ_0 and is mapped to some Pauli by the preparation operation U^{pre}. Then, the (faulty) CNOT gate is applied to the state ρ_1. The readout pulse (if required) is denoted U^{post} and the measurement is denoted M. After U^{post}, the state is equal to M and we thus have $\rho_3 = M$. The details for the specific values for each experiments are given in the table below.

Experiment #	ρ_0	U^{pre}	ρ_1	ρ_2	U^{post}	M
1	IZ	$(\pi/2)_2^y$	IX	IX	–	IX
2	IZ	$(\pi/2)_2^{-x}$	IY	ZY	–	ZY
3	IZ	–	IZ	ZZ	$(\pi/2)_2^y$	ZX
4	ZI	$(\pi/2)_1^y$	XI	XX	$(\pi/2)_1^{-y}$	ZX
5	ZI	$(\pi/2)_1^{-x}$	YI	YX	$(\pi/2)_1^x$	ZX
6	ZI	–	ZI	ZI	$(\pi/2)_1^y$	XI
7	ZZ	$(\pi/2)_1^y(\pi/2)_2^y$	XX	XI	–	XI
8	ZZ	$(\pi/2)_1^y(\pi/2)_2^{-x}$	XY	YZ	–	YZ
9	ZZ	$(\pi/2)_1^y$	XZ	$-YY$	$(\pi/2)_2^{-x}$	YZ
10	ZZ	$(\pi/2)_1^{-x}(\pi/2)_2^y$	YX	YI	–	YI
11	ZZ	$(\pi/2)_1^{-x}(\pi/2)_2^{-x}$	YY	$-XZ$	–	$-XZ$
12	ZZ	$(\pi/2)_1^{-x}$	YZ	XY	$(\pi/2)_2^x$	XZ
13	ZZ	$(\pi/2)_2^y$	ZX	ZX	–	ZX
14	ZZ	$(\pi/2)_2^{-x}$	ZY	IY	–	IY
15	ZZ	–	ZZ	IZ	$(\pi/2)_2^y$	IX

In practice, we also need to take reference spectra and label them so that we can remember which reference spectra should be used. In this experiment, the identity pulses are implemented and have the same length as the other pulses.

Discuss initial state preparation and give the results and give single gate benchmarking

Conclusion

Bibliography

[1] M. H. Levitt. *Spin Dynamics: Basics of Nuclear Magnetic Resonance*. 2nd edition, John Wiley & Sons Ltd, 2008.

[2] I. S. Oliveira, T. J. Bonagamba, R. S. Sarthour, J. C. C. Freitas, and E. R. deAzevedo. *NMR Quantum Information Processing*. Elsevier, 2007.

[3] N. Khaneja, T. Reiss, C. Kehlet, T. Schulte-Herbruggen, and S. J. Glaser. Optimal Control of Coupled Spin Dynamics: Design of NMR Pulse Sequences by Gradient Ascent Algorithms. *Journal of Magnetic Resonance*, 172:296-305, 2005.

[4] J. Dodd, M. Nielsen, M. Bremner, and R. Thew. Universal quantum computation and simulation using any entangling hamiltonian and local unitaries. *Physical Review A*, 65(4):040301, 2002.

[5] C. A. Ryan. *Characterization and Control in Large Hilbert Spaces*. PhD thesis, University of Waterloo, 2008.

[6] M. Nielsen, and I. Chuang. *Quantum Computation and Quantum Information*. Cambridge University Press, 2000.

[7] E. M. Fortunato, M. A. Pravia, N. Boulant, G. Teklemariam, T. F. Havel, and D. G. Cory. Design of strongly modulating pulses to implement precise effective Hamiltonians for quantum information processing. *Journal of Chemical Physics*, 116:7599, 2002.

[8] N. Suryaprakash. Structure of molecules by NMR spectroscopy using liquid crystal solvents. *Concepts in Magnetic Resonance*, 10(3):167-192, 1998.

[9] J. W. Emsley, and J. C. Lindon. *NMR Spectroscopy using Liquid Crystal Solvents*. Pergamon Press, 1975.

[10] S. Castellano, and A. A. Bothner-By. Analysis of NMR Spectra by Least Squares. *Journal of Chemical Physics*, 41(12):3863, 1964.

[11] T. S. Mahesh, and D. Suter. Quantum-information processing using strongly dipolar coupled nuclear spins. *Physical Review A*, 74(6):062312, 2006.

[12] S. Arumugam, A. C. Kunwar, and C. L. Khetrapal. NMR spectrum of benzo[b]furan in a nematic phase. *Organic Magnetic Resonance*, 18(3):157-158, 1982.

[13] S. Berger, and S. Braun. *200 and more NMR experiments*. Wiley-VCH, 2004.

[14] P. Diehl, H. P. Kellerhals, and E. Lustig. *NMR Basic Principles and Progress*, vol. 6. Springer-Verlag, 1972.

[15] J. Vogt. *ASPECT 2000 NMR simulation/iteration PANIC*. Bruker Report, part 3:23-25, 1979.

[16] P. Diehl, H. P. Kellerhals, and W. Niederberger. The structure of toluene as determined by NMR of oriented molecules. *Journal of Magnetic Resonance*, 4(3):352-357, 1971.

[17] S. S. Golotvin, and V. A. Chertkov. Pattern recognition of the multiplet structure of NMR spectra. *Russian Chemical Bulletin* (English Translation), 46(3):423-430, 1997.

[18] O. Manscher, K. Schaumburg, and J. P. Jacobsen. A Discussion of the Error Analysis in LAOCOON-like Iterative Programs. *Acta Chemica Scandinavia*, A35:13-24, 1981.

[19] P. Diehl, S. Sýkora, and J. Vogt. Automatic analysis of NMR spectra: An alternative approach. *Journal of Magnetic Resonance*, 19(1):67-82, 1975.

[20] R. Laatikainen. Automated analysis of NMR spectra. *Journal of Magnetic Resonance*, 92(1):1-9, 1991.

[21] R. Laatikainen. Dipolar coupling and solvent dependence of 1H, 1H spin-spin coupling in naphthalene. analysis of spectra containing overlapping lines. *Journal of Magnetic Resonance*, 78(1):127-132, 1988.

[22] C. Glidewell, D. W. H. Rankin, and G. M. Sheldrick. Analysis of the proton magnetic resonance spectra of phenol and thiophenol and their methyl, silyl and germyl derivatives. *Transaction of the Faraday Society*, 65:2801-2805, 1969.

[23] J. Heinzer. Iterative least-squares nmr lineshape fitting with use of symmetry and magnetic equivalence factorization. *Journal of Magnetic Resonance*, 26(2):301-316, 1977.

[24] D. S. Stephenson, and G. Binsch. Automated analysis of high-resolution NMR spectra. I. Principles and computational strategy. *Journal of Magnetic Resonance*, 37(3):395-407, 1980.

[25] D. S. Stephenson, and G. Binsch. The molecular structure of cyclopentene in solution as obtained from a nematic phase proton N.M.R. study. *Molecular Physics*, 43(3):697-710, 1981.

[26] G. Hägele, M. Engelhardt, and W. Boenigk. *Simulation und Automatisierte Analyse von Kernresonanzspectren*. VCH, 1987.

[27] V. N. Zinin, A. V. Il'yasov, U. Weber, G. Hägele, and H. Thiele. The 19F NMR spectrum of bis-trifluoromethylmercury Hg(CF3)2 in the nematic phase: DAISY - a novel program system for the analysis and simulation of NMR spectra. *Journal of Fluorine Chemistry*, 70(2):289-292, 1995.

[28] S. V. Zubkov, and V. A. Chertkov. Experimental Determination of Pseudorotation Potentials for Disubstituted Cyclopentanes Based on Spin-Spin Coupling Constants. *International Journal of Molecular Sciences*, 4(3):107-118, 2003.

[29] H. Takeuchi, K. Inoue, Y. Ando, and S. Konaka. Efficient Method to Analyze NMR Spectra of Solutes in Liquid Crystals: The Use of Genetic Algorithm and Integral Curves. *Chemical Letters*, 11:1300-1301, 2000.

[30] J. A. Hageman , R. Wehrens, R. de Gelder, W. Leo Meerts, and L. M. C. Buydens. Direct determination of molecular constants from rovibronic spectra with genetic algorithms. *Journal of Chemical Physics*, 113(18):7955, 2000.

[31] W. Leo. Meerts, C. A. de Lange, A. C. J. Weber, and E. E. Burnell. A simple two-step automatic assignment procedure for complicated NMR spectra of solutes in liquid crystals using genetic algorithms. *Chemical Physics Letters*, 441:342-346, 2007.

[32] Ronald Y. Dong. *Nuclear magnetic resonance spectroscopy of liquid crystals*. World Scientific Publishing Company, 2009.

[33] W. Leo. Meerts, C. A. de Lange, A. C. J. Weber, and E. E. Burnell. Evolutionary algorithms to solve complicated NMR spectra. *Journal of Chemical Physics*, 130(4):044504, 2009.

[34] H. Oschkinat, A. Pastore, P. Pfändler, and G. Bodenhausen. Two-dimensional correlation of directly and remotely connected transitions by z-filtered COSY. *Journal of Magnetic Resonance*, 69(3):559-566, 1986.

[35] R. C. R. Grace, N. Suryaprakash, A. Kumar, and C. L. Khetrapal. Application of a Modified Z-COSY Experiment for the Analysis of Spectra of Oriented Molecules - The Spectrum of cis,cis-Mucanonitrile. *Journal of Magnetic Resonance*, 107(1):79-82, 1994.

[36] P. Mansfield. Symmetrized pulse sequences in high resolution NMR in solids. *Journal of Physics C*, 4(11):1444, 1971.

[37] P. Mansfield, M. J. Orchard, D. C. Stalker, and K. H. B. Richards. Symmetrized Multipulse Nuclear-Magnetic-Resonance Experiments in Solids: Measurement of the Chemical-Shift Shielding Tensor in Some Compounds. *Physical Review B*, 7(1):90-105, 1973.

[38] W.-K. Rhim, D. D. Elleman, and R.W. Vaughan. Analysis of multiple pulse NMR in solids. *Journal of Chemical Physics*, 59(7):3740, 1973.

[39] M. K. Henry, C. Ramanathan, J. S. Hodges, C. A. Ryan, M. J. Ditty, R. Laflamme, and D. G. Cory. Fidelity Enhancement by Logical Qubit Encoding. *Physical Review Letters*, 99(22):220501, 2007.

[40] J. Zhang, M. Ditty, D. Burgarth, C. A. Ryan, C. M. Chandrashekar, M. Laforest, O. Moussa, J. Baugh, and R. Laflamme. Quantum data bus in dipolar coupled nuclear spin qubits. *Physical Review A*, 80(1):012316, 2009.

[41] L. D. Field. Multiple Quantum NMR of Partially Aligned Molecules. *Annual Reports on NMR Spectroscopy*, 59:1-39, 2006.

[42] B. Baishya, and N. Suryaprakash. Spin State Selective Detection of Single Quantum Transitions Using Multiple Quantum Coherence : Simplifying the Analyses of Complex NMR Spectra. *Journal of Physical Chemistry A*, 111:5211-5217, 2007.

[43] D. Burgarth, K. Maruyama, and F. Nori. Coupling strength estimation for spin chains despite restricted access. *Physical Review A*, 79(2):020305(R), 2009.

[44] K. Maruyama, D. Burgarth, A. Ishizaki, K. B. Whaley, and T. Takui. Hamiltonian tomography of dissipative systems under limited access: A biomimetic case study. arXiv:1111.1062v1 [quant-ph].

[45] E. H. Lapasar, K. Maruyama, D. Burgarth, T. Takui, Y. Kondo, and M. Nakahara. stimation of Coupling Constants of a Three-Spin Chain: Case Study of Hamiltonian Tomography with NMR. arXiv:1111.1381v1 [quant-ph].

[46] J. Nocedal, and S. J. Wright. *Numerical Optimization*. 2nd edition, Springer, 2006.

[47] C. Audet, and J. E. Dennis Jr. Analysis of Generalized Pattern Searches. *SIAM Journal of Optimization*, 13(3):889-903, 2003.

[48] T. F. Coleman, and Y. Li. An Interior Trust Region Approach for Nonlinear Minimization Subject to Bounds. *SIAM Journal of Optimization*, 6(2):418-445, 1996.

[49] A. J. Shaka, P. B. Barker, and R. Freeman. Computer-optimized decoupling scheme for wideband applications and low-level operation. *Journal of Magnetic Resonance*, 64(3):547-552, 1985.

[50] T. Bräuniger, P. Wormald, and P. Hodgkinson. Improved proton decoupling in NMR spectroscopy of crystalline solids using the SPINAL-64 sequence. *Monatshefte für Chemie*, 133(2):1549-1554, 2002.

[51] C. B. Moler, and G. W. Stewart. An Algorithm for Generalized Matrix Eigenvalue Problems. *SIAM Journal on Numerical Analysis*, 10(2):241-256, 1973.

[52] R. G. Mavinkurve, H. S. V. Deepak, K. V. Ramanathan, and N. Suryaprakash. Analyses of the complex proton NMR spectra: Determination of anisotropic proton

chemical shifts of oriented molecules by a two dimensional experiment. *Journal of Magnetic Resonance*, 185(2):240-246, 2007.

[53] M. Lee, and W. I. Goldburg. Nuclear-Magnetic-Resonance Line Narrowing by a Rotating rf Field. *Physical Review A*, 140(4):1261-1271, 1965.

[54] I. L. Chuang, and M. A. Nielsen. Prescription for experimental determination of the dynamics of a quantum black box. *Journal of Modern Optics*, 44(11):2455-2467, 1997.

[55] J. Emerson, R. Alicki, and K. Zyczkowski. Scalable noise estimation with random unitary operators. *J. Opt. B: Quantum and Semiclassical Optics*, 7:S347-S352, 2005.

[56] C. Dankert, R. Cleve, J. Emerson, and E. Livine. Exact and approximate unitary 2-designs: constructions and applications. *Physical Review A*, 80(1):012304, 2009.

[57] M. P. da Silva. *Suppression and characterization of decoherence in practical quantum information processing devices*. PhD thesis, University of Waterloo, 2008.

[58] O. Moussa, M. P. da Silva, C. A. Ryan, and R. Laflamme. Practical experimental certification of computational quantum gates using a Twirling procedure. *Physical Review Letters*, 109(7):070504, 2012.

[59] J. Emerson, M. P. da Silva, O. Moussa, C. A. Ryan, M. Laforest, J. Baugh, D. G. Cory, R. Laflamme. Symmetrized characterization of noisy quantum processes. *Science*, 317(5846):1893-1896, 2007.

[60] S. S. Venkatesh. *The Theory of Probability: Explorations and Applications*. Cambridge University Press, 2012.